Compact Q-switched 2 μm Tm:$GdVO_4$ laser with MoS_2 absorber

Pingguang Ge, Jie Liu,* Shouzhen Jiang, Yuanyuan Xu, and Baoyuan Man

Shandong Provincial Key Laboratory of Optics and Photonic Device, School of Physics and Electronics, Shandong Normal University, Jinan 250014, China

**Corresponding author: jieliu@sdnu.edu.cn*

Received June 17, 2015; revised July 30, 2015; accepted August 4, 2015; posted August 5, 2015 (Doc. ID 243066); published August 31, 2015

A molybdenum disulfide (MoS_2) saturable absorber was fabricated by thermally decomposing the ammonium thiomolybdate. By using the MoS_2 absorber, a compact diode-pumped passively Q-switched Tm:$GdVO_4$ laser has been demonstrated. A stable Q-switched laser with repetition rates from 25.58 to 48.09 kHz was achieved. Maximum average output power was 100 mW with the shortest pulse duration of 0.8 μs. Maximum pulse energy is 2.08 μJ at center of 1902 nm.

OCIS codes: (140.3540) Lasers, Q-switched; (140.3580) Lasers, solid-state; (160.4330) Nonlinear optical materials.

http://dx.doi.org/10.1364/PRJ.3.000256

1. INTRODUCTION

Two-dimensional (2D) nanomaterials have attracted much attention recently due to their remarkable electronic and optical properties. A well-known 2D nanomaterial, graphene, has been widely investigated as an excellent saturable absorber (SA) for the wavelength range between 0.8 and 3 μm due to its unique zero bandgap, high thermal stability, and the excellent saturable absorption properties [1–5]. With the wide application of graphene-based SAs, other graphene-like 2D materials also have attracted extensive attention. Recently, molybdenum disulfide (MoS_2), a new type of 2D material, transition metal dichalcogenides [6], has received attention due to its thickness-dependent electronic and optical properties. MoS_2 is composed of a hexagonal structure of molybdenum atoms sandwiched between two layers of chalcogen atoms [6]. Reference [7] demonstrated that the MoS_2 has a nonlinear optical response stronger than that of graphene. MoS_2 further has an indirect bandgap of 1.29 eV in bulk form and a direct bandgap of ~1.85 eV in a single layer [8,9]. Because of the direct bandgap of ~1.85 eV in single layer, MoS_2 has a potential application at visible wavelengths [10]. In addition, the few-layer MoS_2 could be regarded as a promising broadband SA for pulsed lasers and has been demonstrated in [11]. Using broadband few-layer MoS_2 as SAs, passively Q-switched and ultrafast lasers have been realized. The 1054 nm passively mode-locked Yb-doped fiber laser and the 1.5 μm passively mode-locked erbium-doped fiber laser were realized by Zhang *et al.* [12] and Xia *et al.* [13], respectively. A passive Q-switching and Q-switched mode-locking Tm:CLNGG laser at a wavelength of 2 μm has been realized [14], from which the minimum pulse duration, maximum output power, and maximum pulse energy of 4.84 μs, 62 mW, and 0.72 μJ were obtained, respectively. In addition, Lou *et al.* reported a fewer-layer MoS_2 dual-wavelength Q-switched Yb:LGGG laser at 1025.2 and 1028.1 nm [15]. A maximum average output power of 0.6 W was obtained, corresponding to single pulse energy up to 1.8 μJ.

Tm:$GdVO_4$ offers many favorable properties [16,17]. The absorption band of that is considerably stronger and broader (770–820 nm) than that in YAG and YAP. Furthermore, the thermal conductivity of $GdVO_4$ is 11.7 $Wm^{-1} K^{-1}$ at 300 K, larger than that in YAP and YLF, which is more efficient cooling the crystal. A maximum output power of 2.6 W at 1910 nm in a diode-pumped continuous wave (CW) Tm:$GdVO_4$ laser had been reported by Cerny *et al.* [18]. An acousto-optical (AO) Q-switch output has also been proved in Tm:$GdVO_4$ [19]. However, a diode-pumped passively Q-switched Tm:$GdVO_4$ laser has not been reported.

In this paper, the MoS_2 SA is fabricated by thermally decomposing ammonium thiomolybdate dip coating the mica and successfully realizing a stable passively Q-switched Tm:$GdVO_4$ laser at 1902 nm. A maximum output power of 100 mW was achieved at 1902 nm, corresponding to the maximum single pulse energy of 2.08 μJ.

2. FABRICATION OF MoS_2 SA

Figure 1 schematically illustrates a convenient and cost-effective approach by thermally decomposing the ammonium thiomolybdate [20]. $(NH_4)_2MoS_4$ (Alfa Aesar, purity of 99.99%; 0.05 g) dissolved into 5 mL organic solvent of dimethylformamide (DMF) to form a uniform and stable solution through sonication for 30 min. We deposited a thin $(NH_4)_2MoS_4$ film onto the fresh surface of mica of just dissociation with a dropper and used a spin coater to ensure uniformity of solution on the mica. The sample should be placed in the hot zone of the furnace for drying naturally horizontally. After this, the annealing process was carried out in the quartz tube. First, the quartz tube was pumped to low pressure accompanied by a flow of H_2 and Ar (20/80 sccm). Subsequently, a temperature of 500°C was kept for an hour in the growth process. Finally,

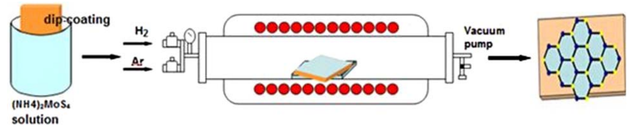

Fig. 1. Schematic illustration of the formation of MoS_2.

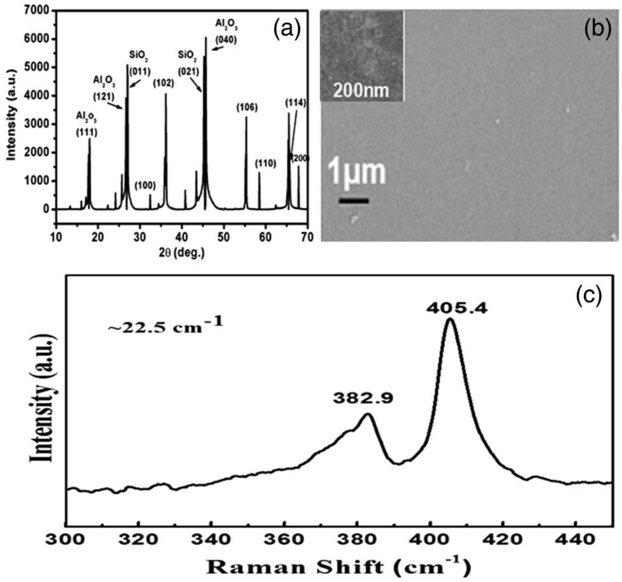

Fig. 2. (a) XRD pattern. (b) SEM images of as-grown MoS_2 on mica substrates. (c) Trilayered MoS_2 Raman spectra.

the furnace was quickly cooled to room temperature by opening the furnace.

The XRD results of exfoliated MoS_2 NPs in Fig. 2(a) are in good fit the hexagonal structure of MoS_2 (PDF Card 04-0880). Several diffraction peaks are easily indexed, assigned to (110), (100), (102), and (106) reflection.

Figure 2(b) exhibits the SEM image of the MoS_2 membrane after the decomposition of ammonium thiomolybdate on mica substrate. A large area continuous MoS_2 layer is obtained. As shown in the SEM image, the surface of the sample is uniform and compliant.

Figure 2(c) shows the Raman spectroscopy on trilayered MoS_2. The characteristic peaks of the two samples at 382.9 and 405.4 cm^{-1} are assigned to the E^1_{2g} and A_{1g} modes of MoS_2, respectively, while the two characteristic peaks E^1_{2g} and A_{1g} of the bulk MoS_2 occur at 380 and 410 cm^{-1} [21]. Compared with the thickness-related distance value of bulk MoS_2 between the two peaks is ~30 cm^{-1}, the thickness-related distance value of the trilayered MoS_2 between the two peaks in ~22.5 cm^{-1}. The frequency difference of the two modes can be used to determine the layer thickness of MoS_2. In our result, the thickness-related distance of ~22.5 cm^{-1} corresponds to three or four layers of MoS_2 [22,23].

3. EXPERIMENT SETUP

A schematic of the experimental arrangement is shown in Fig. 3. A fiber-coupled diode laser was used as the pump resource, whose emission wavelength was around 803 nm at 25.4°C. The pump core diameter and the numerical aperture were 400 μm and 0.22, respectively. By using a couple of convex lens (1:0.5), the pump beam was focused on the laser crystal with the radius of 100 μm. The laser crystal was *a*-cut Tm:$GdVO_4$ crystal with the Tm^{3+} doping concentration of 0.5 at. % and the dimension of 3 mm × 3 mm × 3 mm, which both surfaces were antireflection coating at the pump and laser wavelengths. It was wrapped with an indium foil and then mounted on a water-cooled copper crystal holder with the cooling water temperature set at 15°C to preserve the laser crystal from thermal fracture. The absorption efficiency of the diode pump by the crystal was 77.86%. The input mirror M1 was a plane-concave mirror with radius of 100 mm, which was high-transmission coated at 780–810 nm and high-reflection coated at 1900–2000 nm. A flat mirror M2 with the transmission of 2% was used as the output coupler (OC). A compact concave-plane resonator was designed to keep the mode matching in crystal between the pump beam and the fundamental resonant mode. The laser pulse trains was recorded by a 1 GHz digital oscilloscope (Tektronix DPO 4104) and a fast photodiode detector (ET-5000) with a rising time of 250 ps. The average output power was measured by a laser power meter (30A-SH-V1, made in Israel).

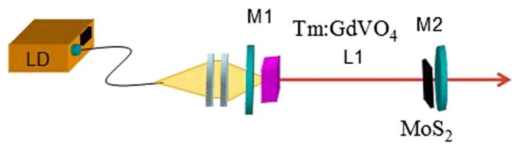

Fig. 3. Schematic configuration of the *Q*-switched Tm:$GdVO_4$ laser.

4. RESULTS AND DISCUSSION

The average output powers of the CW and passively *Q*-switched Tm:$GdVO_4$ laser versus absorbed pump power are shown in Fig. 4. In the CW operation, the laser threshold pumping power was 2.12 W without inserting MoS_2 SA. When the absorbed pump powers were increased to 3.08 W, the maximum output power of 304 mW was obtained with corresponding slope efficiency of 19%. In the passively *Q*-switched operation, the MoS_2 SA was positioned close to the M2. The radius of the laser beam at the MoS_2 SA was

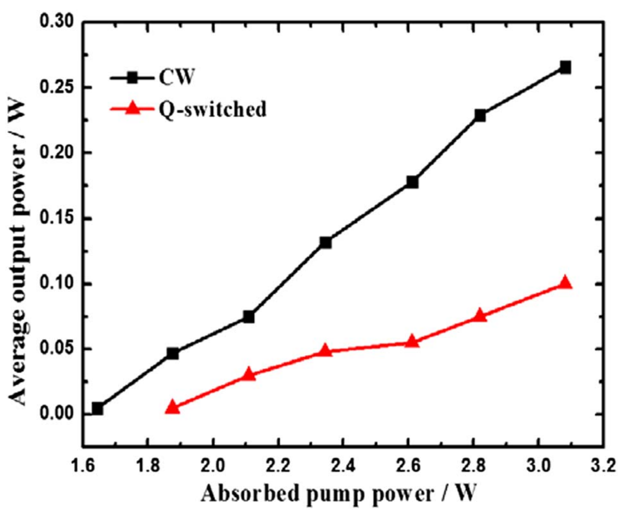

Fig. 4. Average output power of CW and passively *Q*-switched versus the absorbed pump power.

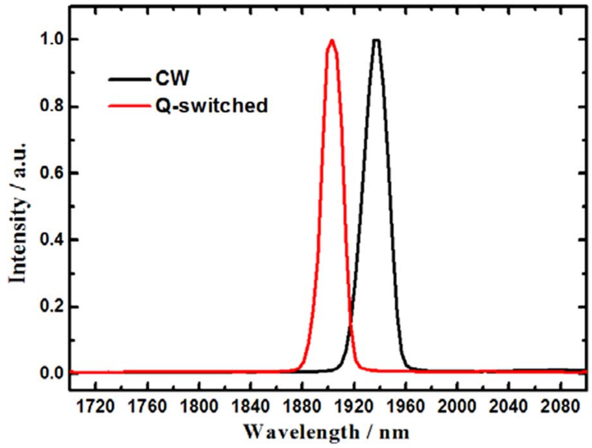

Fig. 5. Output spectra from $Tm:GdVO_4$ lasers in CW operation and passively *Q*-switched operation.

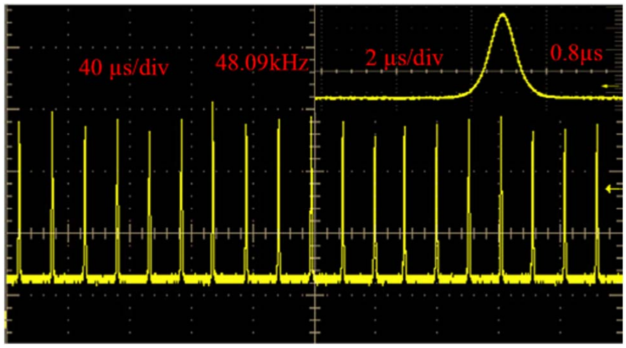

Fig. 7. Passively *Q*-switched pulse at 40 and 2 μs/div.

calculated to be about 125 μm by ABCD matrix. By carefully aligning the laser cavity, the passively *Q*-switched pulse train was searched. The laser threshold pumping power was 2.41 W. The maximum output power of 100 mW was obtained with a corresponding slope efficiency of 7.3% with the absorbed pump powers of 3.08 W. To avoid damage to the laser crystal and MoS_2, the pump power was not increased more than 4.0 W.

The CW and *Q*-switched pulse spectrum were measured by an optical spectrum analyzer (AvaSpec-NIR256–2.2-RM) with a resolution of 10 nm. Figure 5 shows the CW and *Q*-switched spectra under the absorbed pump power of 3.08 W. We can see the central wavelengths were 1938 and 1902 nm. The central wavelength of *Q*-switching was shorter than that of the CW, which was attributed to the stimulated emission cross section in the *Q*-switched operation becoming a key factor because the energy stored in the crystal far exceeds the CW operation threshold [24].

The pulse width and the repetition rate of the passively *Q*-switched operation as the function of the absorbed pump power are shown in Fig. 6. It can be seen that the repetition increases as the pulse width decreases rapidly. In Fig. 6, we can see that, when the absorbed pump power is increased from 1.88 to 3.08 W, the pulse duration decreased from 2 to 0.8 μs with the pulse repetition rate increasing from 25.58 to 48.09 kHz. The maximum repetition rate of 48.09 kHz and the minimum pulse width of 0.8 μs were achieved under the absorbed pump power of 3.08 W, corresponding to the maximum single pulse energy of 2.08 μJ.

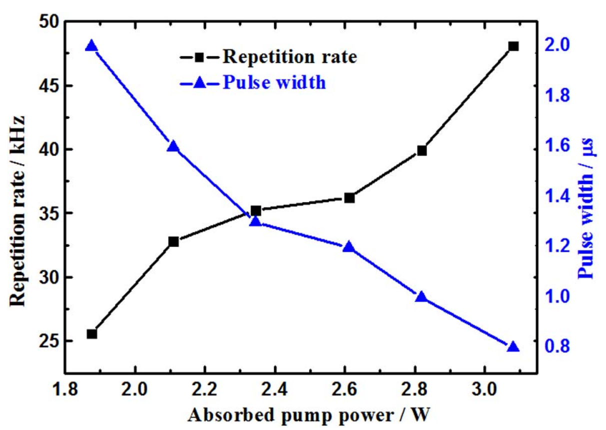

Fig. 6. Pulse width and repetition rate as a function of absorbed pump power.

Figure 7 gives a recorded typical oscilloscope pulse train with the time of 40 and 2 μs/div. The experimental result was obtained at the absorbed pump power of 3.08 W. The pulse-to-pulse amplitude fluctuation of the *Q*-switched pulse train was less than 5%. In order to protect the laser crystal and MoS_2 from damage, we no longer increased the pump power. In future experiments, we will continue to optimize cavity type to obtain excellent *Q*-switching stability and *Q*-switch mode-lock.

5. CONCLUSIONS

In conclusion, using a MoS_2 as a SA, which was fabricated by thermally decomposing the ammonium thiomolybdate, a passively *Q*-switched $Tm:GdVO_4$ laser was realized. A maximum output power of 100 mW and pulse duration of 0.8 μs were achieved at 1902 nm, corresponding to the slope efficiency of 7.3%, and the single pulse energy was 2.08 μJ. As far as we know, this is the first report on diode-pumped passively *Q*-switched $Tm:GdVO_4$ lasers with the MoS_2. With further optimization of the MoS_2-SA, the higher output power and CW mode-locking laser performance can be anticipated.

ACKNOWLEDGMENT

The authors acknowledge support from the National Natural Science Foundation of China (nos. 61475089, 61205174, 11474187), the development projects of Shandong Province Science and Technology, and Excellent Young Scholars Research Fund of Shandong Normal University.

REFERENCES

1. J. L. Xu, X. L. Li, J. L. He, X. P. Hao, Y. Z. Wu, Y. Yang, and K. J. Yang, “Performance of large-area few-layer graphene saturable absorber in femtosecond bulk laser,” Appl. Phys. Lett. **99**, 261107 (2011).
2. J. Liu, Y. G. Wang, Z. S. Qu, L. H. Zheng, L. B. Su, and J. Xu, “Graphene oxide absorber for 2 μm passive mode-locking $Tm:YAlO_3$ laser,” Laser Phys. Lett. **9**, 15–19 (2012).
3. M. N. Cizmeciyan, J. W. Kim, S. Bae, B. H. Hong, F. Rotermund, and A. Sennaroglu, “Graphene mode-locked femtosecond Cr:ZnSe laser at 2500 nm,” Opt. Lett. **38**, 341–343 (2013).

4. Z. Sun, T. Hasan, F. Torrisi, D. Popa, G. Privitera, F. Wang, F. Bonaccorso, D. M. Basko, and A. C. Ferrari, "Graphene mode-locked ultrafast laser," ACS Nano **4**, 803–810 (2010).
5. S. Tokita, M. Murakami, S. Shimizu, M. Hashida, and S. Sakabe, "Graphene Q-switching of a 3 μm Er:ZBLAN fiber laser," in *Advanced Solid-State Lasers Congress* (2013), paper AF2A.9
6. Q. H. Wang, K. Kalantar-Zadeh, A. Kis, J. N. Coleman, and M. S. Strano, "Electronics and optoelectronics of two-dimensional transition metal dichalcogenides," Nat. Nanotechnol. **7**, 699–712 (2012).
7. K. P. Wang, J. Wang, J. T. Fan, M. Lotya, A. O'Neill, D. Fox, Y. Y. Feng, X. Y. Zhang, B. X. Jiang, Q. Z. Zhao, H. Z. Zhang, J. N. Coleman, L. Zhang, and W. Josef, "Ultrafast saturable absorption of two-dimensional MoS_2 nanosheets," ACS Nano **7**, 9260–9267 (2013).
8. K. F. Mak, C. Lee, J. Shan, and T. F. Heinz, "Atomically thin MoS_2: a new direct-gap semiconductor," Phys. Rev. Lett. **105**, 136805 (2010).
9. R. L. Woodward, R. C. T. Howe, G. Hu, F. Torrisi, M. Zhang, T. Hasan, and E. J. R. Kelleher, "Few-layer MoS_2 saturable absorbers for short-pulse laser technology: current status and future perspectives invited," Photon. Res. **3**, A30–A42 (2015).
10. K. Wang, J. Wang, J. Fan, and M. Lotya, "Ultrafast saturable absorption of two-dimensional MoS_2 nanosheets," ACS Nano **7**, 9260–9267 (2013).
11. S. Wang, H. Yu, H. Zhang, A. Wang, M. Zhao, Y. Chen, L. Mei, and J. Wang, "Broadband few-layer MoS_2 saturable absorber," Adv. Mater. **26**, 3538–3544 (2014).
12. H. Zhang, S. B. Lu, J. Zheng, J. Du, S. C. Wen, D. Y. Tang, and K. P. Loh, "Molybdenum disulfide (MoS_2) as a broadband saturable absorber for ultra-fast photonics," Opt. Express **22**, 7249–7260 (2014).
13. H. D. Xia, H. P. Li, C. Y. Lan, C. Li, X. X. Zhang, S. J. Zhang, and Y. Liu, "Ultrafast erbium-doped fiber laser mode-locked by a CVD grown molybdenum disulfide (MoS_2) saturable absorber," Opt. Express **22**, 17341–17348 (2014).
14. L. C. Kong, G. Q. Xie, P. Yuan, L. J. Qian, S. X. Wang, H. H. Yu, and H. J. Zhang, "Passive Q-switching and Q-switched mode-locking operations of 2 μm Tm:CLNGG laser with MoS_2 saturable absorber mirror," Photon. Res. **3**, A47–A50 (2015).
15. F. Lou, R. Zhao, J. He, Z. Jia, X. Su, Z. Wang, J. Hou, and B. Zhang, "Nanosecond-pulsed, dual-wavelength, passively Q-switched ytterbium-doped bulk laser based on few-layer MoS_2 saturable absorber," Photon. Res. **3**, A25–A29 (2015).
16. Y. Urata, K. Akagawa, S. Wada, H. Tashiro, S. J. Suh, D. H. Yoon, and T. Fukuda, "Growth and optical properties of Tm:$GdVO_4$ single crystal," Cryst. Res. Technol. **34**, 41–45 (1999).
17. Y. F. Li, Y. Z. Wang, and B. Q. Yao, "Comparative optical study of thulium-doped $YAlO_3$ and $GdVO_4$ single crystals," Laser Phys. Lett. **5**, 37–40 (2008).
18. P. Cerny, J. Oswald, J. Sulc, H. Jelinkova, Y. Urata, and M. Higuchi, "Multi-watt and tunable diode-pumped operation of Tm:$GdVO_4$ crystal grown by a floating zone method," in *Advanced Solid State Photonics* (2006).
19. Z. G. Wang, C. W. Song, Y. F. Li, Y. L. Ju, and Y. Z. Wang, "CW and pulsed operation of a diode-end-pumped Tm:$GdVO_4$ laser at room temperature," Laser Phys. Lett. **6**, 105–108 (2009).
20. K. K. Liu, W. J. Zhang, Y. H. Lee, Y. C. Lin, M. T. Chang, C. Y. Su, C. S. Chang, H. Li, Y. M. Shi, H. Zhang, C. S. Lai, and L. J. Li, "Growth of large-area and highly crystalline MoS_2 thin layers on insulating substrates," Nano Lett. **12**, 1538–1544 (2012).
21. B. Xu, Y. J. Cheng, Y. Wang, Y. Z. Huang, J. Peng, Z. Q. Luo, H. Y. Xu, Z. P. Cai, J. Weng, and R. Moncorgé, "Passively Q-switched Nd:$YAlO_3$ nanosecond laser using MoS_2 as saturable absorber," Opt. Express **22**, 28934–28940 (2014).
22. Y. Yu, C. Li, Y. Liu, L. Su, Y. Zhang, and L. Cao, "Controlled scalable synthesis of uniform, high-quality monolayer and few-layer MoS_2 films," Sci. Rep. **3**, 1–5 (2013).
23. Y. Lee, J. Lee, H. Bark, I.-K. Oh, G. H. Ryu, Z. Lee, H. Kim, J. H. Cho, J.-H. Ahn, and C. Lee, "Synthesis of wafer-scale uniform molybdenum disulfide films with control over the layer number using a gas phase sulfur precursor," Nanoscale **6**, 2821–2826 (2014).
24. S. Shu, T. Yu, J. Hou, R. Liu, M. Huang, and W. Chen, "End-pumped all solid-state high repetition rate Tm, Ho:LuLF laser," Chin. Opt. Lett. **9**, 021401 (2011).